

1995127388

TERRAIN CLASSIFICATION USING CIRCULAR POLARIMETRIC FEATURES

David G. Michelson and Ian G. Cumming
University of British Columbia, Vancouver, B.C., Canada V6T 1Z4
E-mail: davem@ee.ubc.ca and ianc@ee.ubc.ca

Charles E. Livingstone
Canada Centre for Remote Sensing, Ottawa, Ont., Canada K1A 0Y7
E-mail: livingstone@ccrs.emr.ca

1 Introduction

Conventional representations of polarization response are referred to a horizontally and vertically polarized basis. Recent studies by Freeman and Durden [1], van Zyl [2], and others suggest that alternative polarimetric features which more easily resolve the contributions of simple scattering mechanisms such as odd-bounce, even-bounce, and diffuse scattering could offer several advantages in terrain classification. The circular polarization covariance matrix is a potential source of such features. In this paper, we derive its relationship to the Stokes matrix, describe some of its properties, and compare the utility of linear and circular polarimetric features in classifying an AIRSAR scene containing urban, park, and ocean terrain.

2 Properties of the Circular Polarization Covariance Matrix

In the monostatic case, the circular polarization covariance matrix $[C]$ is given in terms of the elements of the circular polarization scattering matrix, $S_{\ell\ell}$, $S_{\ell r}$, $S_{r\ell}$, and S_{rr} , by the reduced form

$$[C] = \begin{bmatrix} \langle S_{\ell\ell} S_{\ell\ell}^* \rangle & \langle S_{\ell\ell} S_{\ell r}^* \rangle & \langle S_{\ell\ell} S_{rr}^* \rangle \\ \langle S_{\ell r} S_{\ell\ell}^* \rangle & \langle S_{\ell r} S_{\ell r}^* \rangle & \langle S_{\ell r} S_{rr}^* \rangle \\ \langle S_{rr} S_{\ell\ell}^* \rangle & \langle S_{rr} S_{\ell r}^* \rangle & \langle S_{rr} S_{rr}^* \rangle \end{bmatrix}, \quad (1)$$

where, by definition, $S_{\ell r} = S_{r\ell}$. In this format, the polarization responses of odd-bounce, even-bounce, and diffuse scatterers are given by

$$[C_o] = \begin{bmatrix} 0 & 0 & 0 \\ 0 & 1 & 0 \\ 0 & 0 & 0 \end{bmatrix}, \quad [C_e] = \begin{bmatrix} 1 & 0 & 1 \\ 0 & 0 & 0 \\ 1 & 0 & 1 \end{bmatrix}, \quad [C_d] = \begin{bmatrix} 1 & 0 & 0 \\ 0 & 1 & 0 \\ 0 & 0 & 1 \end{bmatrix}, \quad (2)$$

respectively. It can be shown that the representation of the target response after rotation of the target by an angle α is given by

$$[C'] = \begin{bmatrix} S_{\ell\ell} S_{\ell\ell}^* & S_{\ell\ell} S_{\ell r}^* e^{-j2\alpha} & S_{\ell\ell} S_{rr}^* e^{-j4\alpha} \\ S_{\ell r} S_{\ell\ell}^* e^{j2\alpha} & S_{\ell r} S_{\ell r}^* & S_{\ell r} S_{rr}^* e^{-j2\alpha} \\ S_{rr} S_{\ell\ell}^* e^{j4\alpha} & S_{rr} S_{\ell r}^* e^{j2\alpha} & S_{rr} S_{rr}^* \end{bmatrix} \quad (3)$$

The diagonal elements and the magnitude of the off-diagonal elements are both invariant under rotation of either the target or the radar antenna about the line-of-sight.

In order to derive an expression for the elements of the circular polarization covariance matrix in terms of the elements of the Stokes matrix, it is necessary to express the Stokes vector \mathbf{J} with respect to a circularly polarized basis. Thus,

$$\mathbf{J} = \begin{bmatrix} E_l E_l^* + E_r E_r^* \\ E_l E_r^* + E_r E_l^* \\ j(E_l E_r^* - E_r E_l^*) \\ E_l E_l^* - E_r E_r^* \end{bmatrix} = \begin{bmatrix} |E_l|^2 + |E_r|^2 \\ 2\Re(E_l E_r^*) \\ 2\Im(E_l E_r^*) \\ |E_l|^2 - |E_r|^2 \end{bmatrix} = \begin{bmatrix} a_l^2 + a_r^2 \\ 2a_l a_r \cos \delta_c \\ 2a_l a_r \sin \delta_c \\ a_l^2 - a_r^2 \end{bmatrix}. \quad (4)$$

where $E_l = a_l e^{j\delta_l}$ and $E_r = a_r e^{j\delta_r}$ are the complex amplitudes of the left and right circularly polarized components of the electric field, respectively, and $\delta_c = \delta_r - \delta_l$ is the circular polarimetric phase difference. A derivation similar to that employed by van Zyl and Ulaby [3] for the linearly polarized case yields expressions for the elements of the circular polarization covariance matrix in terms of the elements of the Stokes matrix:

$$\begin{aligned} S_{ll} S_{ll}^* &= a_{11} + 2a_{14} + a_{44}, \\ S_{rr} S_{rr}^* &= a_{11} - 2a_{14} + a_{44}, \\ S_{lr} S_{lr}^* &= a_{11} - a_{44}, \\ S_{ll} S_{rr}^* &= (a_{22} - a_{33}) - j2a_{23}, \\ S_{lr} S_{rr}^* &= (a_{12} - a_{24}) - j(a_{13} - a_{34}), \\ S_{ll} S_{lr}^* &= (a_{12} + a_{24}) - j(a_{13} + a_{34}). \end{aligned} \quad (5)$$

For scattering by azimuthally isotropic terrain, symmetry dictates that the ensemble average of the cross-products of the co-polarized (HH and VV) and the cross-polarized (HV) elements of the linear polarization scattering matrix will be zero, as noted by Borgeaud *et al.* [4] and van Zyl [5]. In this case, the corresponding linear polarization covariance matrix has dimensionality of five. It can be shown that the equivalent circular polarization covariance matrix is given by

$$[C] = \begin{bmatrix} S_{ll} S_{ll}^* & S_{ll} S_{lr}^* & S_{ll} S_{ll}^* \\ S_{lr} S_{ll}^* & S_{lr} S_{lr}^* & S_{lr} S_{ll}^* \\ S_{ll} S_{ll}^* & S_{ll} S_{lr}^* & S_{ll} S_{ll}^* \end{bmatrix} = \begin{bmatrix} A & C - jD & A \\ C + jD & B & C + jD \\ A & C - jD & A \end{bmatrix}, \quad (6)$$

where

$$\begin{aligned} A &= a_{11} + a_{44}, \\ B &= a_{11} - a_{44}, \\ C &= a_{12}, \\ D &= a_{34}. \end{aligned}$$

The quantities A , B , and $|C \pm jD|$ are rotation-invariant. The cross-product $S_{ll} S_{rr}^*$, which is generally a complex quantity, is real in this case. Note that the circular polarization covariance matrix representation of an azimuthally isotropic scatterer has a dimensionality of four.

3 Experimental Results

A comparison of the utility of linear and circular polarimetric features in classifying ground cover and terrain was performed using the May 15, 1985 L-band AIRSAR image of San Francisco. The near range portion of the image in which the look angle was less than 30 degrees was excluded. Training areas for urban, park, and ocean classes were defined as shown in Figure 1(a). A minimum distance decision rule was used to classify each pixel in the image. The averaging box size for computing the Stokes matrix was 2×2 . In the linearly polarized case, the features used were the total power, $\langle S_{hh} S_{hh}^* \rangle$, $\langle S_{vv} S_{vv}^* \rangle$, $\langle S_{hv} S_{hv}^* \rangle$, $\Re\langle S_{hh} S_{vv}^* \rangle$ and $\Im\langle S_{hh} S_{vv}^* \rangle$. In the

circularly polarized case, the features used in classification were the total power, $\langle S_{\ell\ell}S_{\ell\ell}^* \rangle$, and $\langle S_{\ell r}S_{\ell r}^* \rangle$.

The results of classification are presented in Figure 1 and are summarized in Tables 1 and 2. Although both classifiers were able to distinguish ocean from urban and park with ease, the choice between urban and park was slightly less certain. The linear polarimetric classifier tended to classify more pixels as urban than the circular polarimetric classifier, particularly in the area to the north-west of the Golden Gate Bridge and the western shoreline of the city. Confusion matrices for self-classification of training areas are presented in Table 2. They suggest that the circular polarimetric classifier was more consistent in classifying urban areas than the linear polarimetric classifier and may therefore have provided slightly better classification accuracy.

Table 1: Confusion Matrix for Classification of an AIRSAR Image of San Francisco

		Linear Polarimetric Classifier				
		Class	Unclas.	Urban	Park	Ocean
Circular Polarimetric Classifier	Unclas.	4.3%	0.6%	0.2%	0.0%	
	Urban	0.3%	22.9%	6.0%	0.0%	
	Park	0.1%	3.5%	24.2%	0.7%	
	Ocean	0.4%	0.0%	2.2%	34.6%	

Table 2: Confusion Matrices for Self-Classification of Training Areas

Linear Polarimetric Classifier				Circular Polarimetric Classifier					
		Training Area					Training Area		
Class	Urban	Park	Ocean	Class	Urban	Park	Ocean		
Unclas.	6.6%	0.1%	0.0%	Unclas.	6.7%	0.7%	0.0%		
Urban	63.8%	9.8%	0.0%	Urban	70.5%	9.9%	0.0%		
Park	29.4%	89.4%	0.0%	Park	22.2%	87.6%	0.0%		
Ocean	0.3%	0.8%	100.0%	Ocean	0.7%	1.8%	100.0%		

4 Conclusions

We have defined the circular polarization covariance matrix, derived its relationship to the Stokes matrix, and described some of its properties. These properties include the invariance of the magnitude of its elements with respect to rotation of the sensor or the scatterer about the radar line-of-sight and the form of the response of an azimuthally isotropic scatterer. The results of classifying urban, park, and ocean terrain in an AIRSAR scene of San Francisco using linear and circular polarimetric features have been presented and compared. The next step will be to compare the utility of features derived from the linear and circular polarization covariance matrices in classifying representative scenes of sea ice, boreal forest, and agricultural fields.

References

- [1] A. Freeman and S. Durden, "A three-component scattering model to describe polarimetric SAR data," in *Radar Polarimetry* (H. Mott and W.-M. Boerner, eds.), Proc. SPIE, vol. 1748, pp. 213–224, 1993.

- [2] J. J. van Zyl, "Application of Cloude's target decomposition theorem to polarimetric imaging radar data," in *Radar Polarimetry* (H. Mott and W.-M. Boerner, eds.), Proc. SPIE, vol. 1748, pp. 184-191, 1993.
- [3] J.J. van Zyl and F.T. Ulaby, "Scattering matrix representation for simple targets," in *Radar Polarimetry for Geoscience Applications*, F. T. Ulaby and C. Elachi, eds., Norwood, MA: Artech House, 1990, pp. 17-52.
- [4] M. Borgeaud, R.T. Shin, and J.A. Kong, "Theoretical models for polarimetric radar clutter," *J. Electromag. Waves Applic.*, vol. 1, no. 1, pp. 73-89, 1987.
- [5] J. J. van Zyl, "Unsupervised classification of scattering behavior using radar polarimetry data," *IEEE Trans. Geosci. Remote Sensing*, vol. GE-27, pp. 36-45, Jan. 1989.

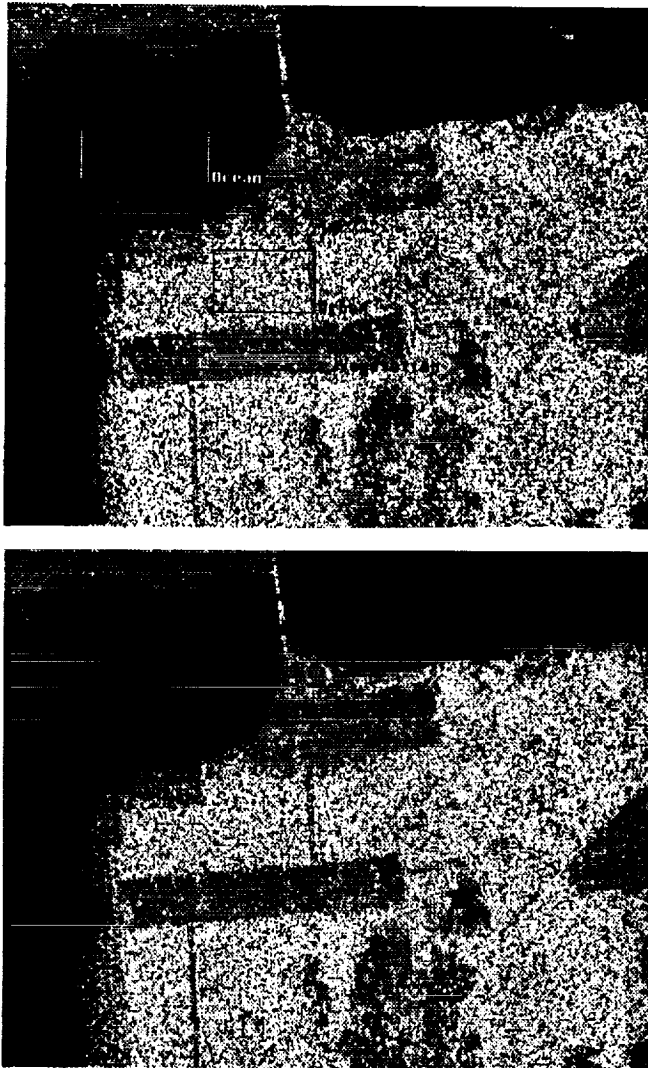


Figure 1: Minimum distance classification of an L-band AIRSAR image of San Francisco using (top) linearly polarized and (bottom) circularly polarized features. Training areas are indicated. Classification legend: urban - white; park - light gray; ocean - black; unclassified - dark gray.